Exoplanets: Detection, Formation and Dynamics
Proceedings IAU Symposium No. 249, 2007
Y.-S. Sun, S. Ferraz-Mello and J.-L. Zhou, eds.

doi:10.1017/S1743921308016797

Planetary migration in gaseous protoplanetary disks

Frédéric S. Masset

Laboratoire AIM, CEA/DSM - CNRS - Université Paris Diderot, DAPNIA/Service d'Astrophysique, CEA/Saclay, 91191 Gif/Yvette Cedex, France, and IA-UNAM, Ciudad Universitaria, Apartado Postal, 70-264, Mexico, D.F. 04510, Mexico

Abstract. Tides come from the fact that different parts of a system do not fall in exactly the same way in a non-uniform gravity field. In the case of a protoplanetary disk perturbed by an orbiting, prograde protoplanet, the protoplanet tides raise a wake in the disk which causes the orbital elements of the planet to change over time. The most spectacular result of this process is a change in the protoplanet's semi-major axis, which can decrease by orders of magnitude on timescales shorter than the disk lifetime. This drift in the semi-major axis is called planetary migration. In a first part, we describe how the planet and disk exchange angular momentum and energy at the Lindblad and corotation resonances. Next we review the various types of planetary migration that have so far been contemplated: type I migration, which corresponds to low-mass planets (less than a few Earth masses) triggering a linear disk response; type II migration, which corresponds to massive planets (typically at least one Jupiter mass) that open up a gap in the disk; "runaway" or type III migration, which corresponds to sub-giant planets that orbit in massive disks; and stochastic or diffusive migration, which is the migration mode of low- or intermediate-mass planets embedded in turbulent disks. Lastly, we present some recent results in the field of planetary migration.

Keywords. planets and satellites: formation, planetary systems: formation, planetary systems: protoplanetary disks

1. Introduction

The importance of the tidal interaction between a protoplanetary disk and a forming planet was first recognized long before the discovery of the first extrasolar planet in 1995. Goldreich & Tremaine (1980) discussed the case of Jupiter in a conservative protoplanetary nebula, and found that its semi-major axis should evolve as a result of the gravitational interaction between the planet and the nebula (although they could not determine whether it should increase or decrease).

When the first extrasolar planet was discovered orbiting 51 Peg with a period of 4.23 days (Mayor *et al.* 1995) at a distance of only 0.052 AU from the central star, theories of orbital migration received renewed attention. None of the reasonable planetary formation scenarios was able to account for the formation of a planetary core that close to the star. It therefore appeared likely that this planet had formed farther out in the protoplanetary disk and then migrated towards the star, along the lines of predictions made by the theoretical work of the eighties (Lin *et al.* 1996).

Had anyone doubted that significant planetary migration is common in forming planetary systems, additional clues were provided by the discovery of planetary systems exhibiting low-order mean motion resonance. Under the effect of differential migration (i.e., the outer planet migrates inwards faster than the inner one), two planets can converge and be captured in a low-order mean motion resonance.

The present contribution is organized as follows: (i) in section 2 we define the notation; (ii) in section 3, we present the torque expressions at the Lindblad and corotation resonances; (iii) in section 4, we present the different migration modes that have been envisaged so far; (iv) finally, in section 5 we present a list of recent results that numerical simulations have recently brought to our knowledge of planet–disk interactions.

2. Notation

We consider a Keplerian gaseous disk with vertical scaleheight $H(r)$, surface density $\Sigma(r)$, kinematic viscosity $\nu(r)$, and orbital frequency $\Omega(r)$, where r is the distance to the central object. We consider a planet with a prograde orbit coplanar to the disk, of mass M_p and orbital frequency Ω_p. Whenever we consider a single azimuthal Fourier component of a given quantity, we denote by m its azimuthal wavenumber.

3. Disk torque at an isolated resonance

The problem of determining the torque between any perturbing potential and the disk, in the linear regime, amounts to determining the torque exerted on the disk by the Fourier components of the potential. Goldreich & Tremaine (1979) have shown that angular momentum exchange between the perturbing potential and the disk occurs only at the Lindblad and corotation resonances. Lindblad resonances correspond to locations in the disk where the perturbing potential's frequency in the matter frame ($\tilde{\omega}(r) = m[\Omega_p - \Omega(r)]$) matches $\pm\kappa(r)$ (the epicyclic frequency). The corotation resonance occurs where the perturbing potential's frequency is zero in the matter frame, that is to say at a radius where the disk material rotates along with the perturbing potential.

3.1. *Torque at a Lindblad resonance*

3.1.1. *Torque expression*

The torque expression at a Lindblad resonance by a single Fourier component of the potential with m-fold symmetry is (Goldreich & Tremaine 1979, Meyer-Vernet & Sicardy 1987, Artymowicz 1993)

$$\Gamma_m = -\frac{m\pi^2\Sigma}{rdD/dr}\left(r\frac{d\Phi_m}{dr} + \frac{2\Omega}{\Omega-\Omega_p}\Phi_m\right)^2, \tag{3.1}$$

where Γ_m is the torque exerted on the disk material by the perturbing potential, $D = \kappa(r)^2 - m^2[\Omega(r)-\Omega_p]^2$ represents a distance to the resonance and $\Phi_m(r)$ is the amplitude of the potential component. In Eq. (3.1), the term in brackets and rdD/dr are both to be evaluated at the resonance location. In a Keplerian disk, rdD/dr is positive at the ILR (Inner Lindblad Resonance, where $\tilde{\omega} = -\kappa$) and negative at the OLR (Outer Lindblad Resonance, where $\tilde{\omega} = +\kappa$). The perturbing potential therefore exerts a negative torque on the disk at the ILR, and a positive torque at the OLR. Newton's third law thus implies that the disk exerts a positive (negative) torque on the perturber at the ILR (OLR).

3.1.2. *Lindblad resonance location*

In order to evaluate the torques given by Eq. (3.1), one has to know the location of the Lindblad resonances. As stated previously, a Lindblad resonance is found where $\tilde{\omega} = \pm\kappa$ (the upper sign stands for the OLR, while the lower sign stands for the ILR). Using the fact that $\kappa = \Omega$ in a Keplerian disk, we obtain: $\Omega(r_{\rm LR}) = \frac{m}{m\pm1}\Omega_p$. Note that owing to pressure effects, the waves launched by the potential components are slightly

https://doi.org/10.1017/S1743921308016797 Published online by Cambridge University Press

offset from the resonance locations. In particular, as $m \to \infty$ the turning point locations tend to pile up at a radius given by: $r = r_c \pm \frac{\Omega}{2A} H$ where $A = (1/2) r\Omega \, d\Omega/dr$ is Oort's first constant. These points of accumulation correspond to the radius at which the flow becomes supersonic in the corotating frame (Goodman & Rafikov 2001). In the case of a Keplerian disk, these points are located $\pm(2/3)H$ away from the corotation radius.

3.2. *Torque at a corotation resonance*

The angular momentum exchange at a corotation resonance and a Lindblad resonance are due to different physical processes. In the latter case the perturbing potential tends to excite epicyclic motion, and the angular momentum deposited is evacuated through pressure-supported waves. On the other hand, these waves are evanescent in the corotation region and therefore unable to remove the angular momentum brought there by the perturber (Goldreich & Tremaine 1979). In the linear regime, the corotation torque exerted by a perturbing potential with m-fold symmetry on the disk is

$$\Gamma_C = \frac{\pi^2 m}{2} \left[\frac{\Phi_m^2}{d\Omega/dr} \frac{d}{dr} \left(\frac{\Sigma}{B} \right) \right]_{r_c}, \tag{3.2}$$

where the term in brackets is to be evaluated at the corotation radius. The corotation torque is thus proportional to the gradient of Σ/B, evaluated at the corotation radius, where B is equal to half the flow vorticity. The corotation torque is therefore proportional to the gradient of the vortensity (ratio of the vorticity to the surface density). The corotation torque is therefore zero in a disk with $\Sigma \propto r^{-3/2}$, such as the minimum mass solar nebula (MMSN).

The physical picture of the flow at a corotation resonance with azimuthal wavenumber m is characterized by a set of m eye-shaped libration islands in which fluid elements move along closed streamlines. The corotation torque is prone to saturation, which can be described as follows: when the disk viscosity is close to zero, the vortensity is conserved along a fluid element's path. The libration of fluid elements redistributes the vortensity within the libration islands. Once the vortensity has been sufficiently stirred up, even an infinitesimally small amount of viscosity suffices to render the vortensity uniform over the whole libration island. The corotation torque then goes to zero (i.e., saturates), because it scales with the vortensity gradient.

In order to avoid saturation, the viscosity must be high enough to prevent the vortensity from becoming uniform over the libration islands. This is possible if the viscous timescale across these islands is smaller than the libration timescale, as shown by Ogilvie & Lubow (2003). In this case, viscous diffusion across the libration islands permanently imposes the large-scale vortensity gradient over the libration islands. Finally, it should be noted that saturation properties cannot be captured by a linear analysis, since saturation requires a finite libration time, and thus a finite resonance width.

4. Planetary migration

4.1. *Type I migration*

We consider the case of a low-mass planet, so that the overall disk response can be treated as a linear superposition of its responses to individual Fourier components of the potential. Each component torques the disk at its Lindblad and corotation resonances. We denote by Γ^m_{ILR} the torque of the m^{th} potential component at its ILR, and adopt similar notation for the torques at the Outer Lindblad Resonance (Γ^m_{OLR}) and corotation resonance (Γ^m_{CR}). The total tidal torque exerted by the disk on the planet, which is equal

https://doi.org/10.1017/S1743921308016797 Published online by Cambridge University Press

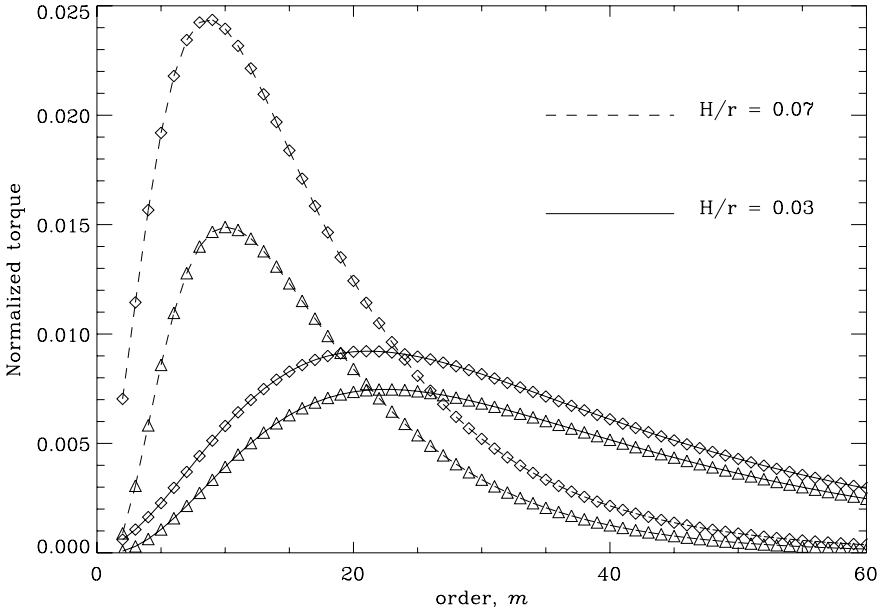

Figure 1. The absolute value of individual inner (triangle) and outer (diamond) torques as a function of m. The torques are normalized to the value $\Gamma_0 = \pi q^2 \Sigma a^4 \Omega_p^2 h^{-3}$, where q is the planet mass to star mass ratio. The one-sided Lindblad torques scale as $(H/r)^{-3}$, hence the total areas under each curve are of the same order of magnitude. The differential Lindblad torque scales as $(H/r)^{-2}$.

and opposite to the torque exerted by the planet on the disk, can therefore be written as

$$\Gamma = \sum_{m>0} \Gamma^m_{ILR} + \sum_{m>0} \Gamma^m_{OLR} + \sum_{m>0} \Gamma^m_{CR}. \tag{4.1}$$

The first series in this sum is the total Inner Lindblad torque, and the second is the total Outer Lindblad torque. The absolute value of either term is also called the one-sided Lindblad torque. The last term is called the coorbital corotation torque. The sum of the two Lindblad torques is referred to as the differential Lindblad torque.

4.1.1. *Differential Lindblad torque*

The acoustic shift of the effective Lindblad resonances mentioned at section 3 has an important consequence: there is a sharp cut-off in the high-m torque components (for $m \gg r/H$) as shown by Artymowicz (1993), since the high-m potential components become localized in increasingly narrow annuli around the perturber orbit. The value of a potential component at the accumulation point (where the torque is exerted) therefore tends to zero as m tends to infinity.

Fig. 1 illustrates the behavior the one-sided Lindblad torques. In particular, one can see that the cutoff occurs at larger m in a thinner disk. Also, for both disk aspect ratios there is a very apparent mismatch between the inner and the outer torques; the former is systematically smaller than the later. If we consider the torque of the disk acting on the planet, then the outer torque is negative and the inner torque is positive; the total torque on the planet is therefore negative. As a consequence, migration is directed inwards and the orbit decays towards the central object (Ward 1986).

https://doi.org/10.1017/S1743921308016797 Published online by Cambridge University Press

4.1.2. *Pressure buffer*

One remarkable feature of the differential Lindblad torque is its weak dependence on the slope of the surface density function. This is not what one would naively expect, since as one increases the slope the surface density increases at the Inner Lindblad Resonances and decreases at the Outer Lindblad Resonances. As one increases the surface density gradient, however, one simultaneously increases the radial pressure gradient. This makes the disk more and more sub-Keplerian. As a consequence, the Outer Lindblad Resonances approach the planet's orbit while the Inner Lindblad Resonances recede from it. This process plays against the more obvious effect of the surface density. This effect is known as the pressure buffer (Ward 1997, Tanaka *et al.* 2002), and frustrates any reasonable attempt to revert the differential Lindblad torque by tuning the power law indexes of the surface density and temperature profiles. This makes inward type I migration inevitable, at least in disks where the surface density and temperature are power laws of the radius.

4.1.3. *Type I migration timescale*

The most up-to-date estimate of the total (*i.e.* Lindblad plus corotation) tidal torque in the linear regime between a three dimensional disk and a low mass planet is the estimate by Tanaka (2002). It yields a migration timescale of 8×10^5 yrs for an Earth-mass object embedded at 5 AU in the MMSN. This is much shorter than the disk lifetime.

4.2. *Type II migration*

4.2.1. *Shock appearance and horseshoe asymmetry*

The wake excited by a planet eventually turns into a shock. The location at which profile steepening produces a shock depends on the planet mass; the larger the mass, the closer the shock will be to the orbit. For planets above some critical mass, the wake becomes a shock within the excitation region. Under these circumstances, the fluid elements circulating just outside the co-orbital region receive a kick of angular momentum every time they cross the wake. This is represented in Fig. 2. As a consequence horseshoe U-turns are not symmetric. A fluid element initially located inside the libration region thus progressively recedes from the orbit as it performs a sequence of horseshoe U-turns, until it ends up in the inner disk or the outer disk (Lubow *et al.* 1999). The co-orbital region is thereby emptied, and an annular gap eventually appears around the orbit. The timescale for emptying the co-orbital region can readily be estimated from Fig. 2. After each horseshoe U-turn, the distance of a fluid element from the orbit increases by an amount between 10 and 20 %. The characteristic emptying time of the horseshoe region is therefore between 5 and 10 times half the libration time, which is given by $\tau_{\rm lib}/2 = 2\pi a/(3/2)\Omega_p x_s = (2/3)T_o(a/x_s)$. Here we can estimate from the figure that $x_s \approx 0.16$, so $\tau_{\rm lib}/2 \approx 4\ T_0$. In this particular example, the co-orbital region is therefore emptied after about 20 to 40 orbits. This simple estimate also shows that the smaller the planet mass, the longer the gap clearance timescale. Indeed, as the planet mass decreases, the horseshoe region becomes more and more symmetric so that more libration times are needed to get rid of the co-orbital material, while the libration time itself increases. For a 1 M_J planet orbiting in a disk with $H/r = 0.05$, the clearance timescale of the gap is about 100 orbits.

4.2.2. *Accretion*

A planet engaged in type II migration has a mass much larger than the critical mass for runaway gas accretion (Pollack *et al.* 1996). It therefore accretes gas from the nebula at the same time as it migrates. Kley (1999) has devised a scheme to simulate the

https://doi.org/10.1017/S1743921308016797 Published online by Cambridge University Press

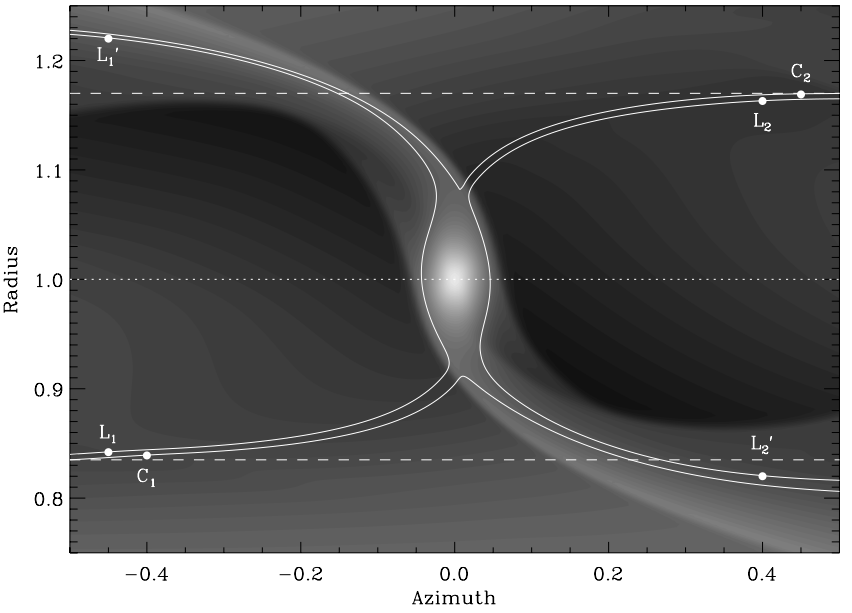

Figure 2. Asymmetry of the horseshoe region. The circulating fluid elements C_2 (moving towards the left) and C_1 (moving towards the right) recede from the orbit after crossing the shock excited by the planet. Similarly, the librating fluid elements recede from the orbit after executing their horseshoe U-turns. This particular example shows streamlines of the flow in the corotating frame of a 2 M_J planet in a disk with $h = 0.05$. The planet is on a fixed circular orbit, and this snapshot was taken after 22.5 orbits.

accretion in the planet's vicinity, and found that a giant planet can still accrete significant amounts of gas despite the presence of the gap. Nelson *et al.* (2000) have found that the final mass of a protogiant of initially one Jupiter mass could be of several Jupiter masses. The ability of a giant planet to accrete the surrounding gas depends on the equation of state of the gas and its ability to get rid of the gravitational energy released by the accretion. D'Angelo *et al.* (2003) and Klahr and Kley (2006) have performed high resolution hydrodynamics calculations taking into account radiative transfer in order to assess the dynamics of the inner Roche lobe and its impact on accretion. They still find significant accretion but the geometry of the flow in the Roche lobe is that of a bubble rather than a thin accretion disk.

4.2.3. *Gap opening criteria*

Classically, the gap opening conditions once consisted of two independent criteria (Lin & Papaloizou 1979, Lin & Papaloizou 1993, Bryden *et al.* 1999) that needed to be simultaneously fulfilled. The first, referred to as the thermal criterion (since it imposes a limit on the disk thickness, and hence on the disk temperature) requires that the wake becomes a shock just as it is excited. The flow must therefore be strongly non-linear in the planet's vicinity, and the parameter R_H/H must be larger than some critical value, where R_H is the planetary Hill radius. This critical value is ~ 1, although its precise value can be slightly different. The second criterion is that the viscosity is sufficiently low, so that the surface density jump across the edges of the excavated region is a sizable fraction of the unperturbed surface density. This condition, which is known as the viscous criterion, is expressed as $q > \frac{40}{\mathcal{R}}$ where $\mathcal{R} = a^2\Omega_p/\nu$ is the Reynolds number.

https://doi.org/10.1017/S1743921308016797 Published online by Cambridge University Press

Crida *et al.* (2006) have used another condition, namely that the circulating streamline just outside the separatrix should be closed, to derive the gap surface density profile semi-analytically. They require that the integral of the viscous, gravitational, and pressure torques cancels out over one synodic period of a given fluid element. They provide an ansatz expression for the pressure torque that is approximately valid for a reasonable range of planetary masses and disk thicknesses, and derive the following unique criterion for gap opening: $\frac{3}{4}\frac{H}{R_H} + \frac{50}{q\mathcal{R}} < 1$. Broadly speaking, this criterion is approximately equivalent to the previous two except in the case where both are only marginally fulfilled.

4.2.4. *Migration of planets that open a gap*

A "clean" gap (i.e., a gap with little residual surface density) splits the disk material into an outer disk and an inner disk. Therefore, the planet must drift inwards at the same rate that the outer disk spreads inwards. In other words, the migration rate of a giant planet that has opened a gap in the disk is the same as the viscous drift rate of the disk (Lin & Papaloizou 1986). This type of migration is referred to as type II migration (Nelson *et al.* 2000 and refs. therein). It is usually said that in this regime, the planet's orbit is locked to the disk's viscous evolution. The migration drift rate of the planet is therefore

$$\frac{da}{dt} \sim -\frac{\nu}{a}. \tag{4.2}$$

For a $M_p = 1\ M_J$ planet that undergoes type II migration in a disk with $H/r = 0.04$ and $\alpha = 6 \cdot 10^{-3}$, the migration time starting from $a = 5$ AU is about $1.6 \cdot 10^4$ orbits. This corresponds to $\sim 1.6 \cdot 10^5$ years, if the central object has one solar mass.

Using two-dimensional numerical simulations, Nelson *et al.* (2000) have shown that the migration of giant planets (with masses greater than or equal to one Jupiter mass) in a viscous disk obeys the scenario outlined above, at least broadly speaking. In particular, they found that the timescale of variation in the planet's semi-major axis is similar to the viscous timescale of the disk. These results have been obtained by assuming that the effective viscosity of the disk is adequately modeled by the Navier–Stokes equation. In this approach the kinematic viscosity is chosen to account for the accretion rates inferred from observations of T Tauri objects. Nelson & Papaloizou (2003) and Papaloizou *et al.* (2004) have performed much more numerically demanding calculations; instead of resorting to the purely hydrodynamical scheme including an *ad hoc* kinematic viscosity, their model describes the self-sustained magnetohydrodynamic (MHD) turbulence arising from the magnetorotational instability (MRI).

They find that a giant protoplanet still opens a gap in the disk, in much the same manner as in a disk modeled by the Navier–Stokes equations. Surprisingly, the gap in a turbulent disk tends to be larger and deeper than in a laminar disk (Papaloizou *et al.* 2007). The mass accretion rate tends to be larger in the MHD turbulent case, most likely because of magnetic breaking of the circumplanetary disk (Papaloizou *et al.* 2004).

4.2.5. *Type II migration of several planets*

The migration properties of two or more giant planets is a topic that has received a lot of attention, primarily because we detect extrasolar giant planets that are in mean motion resonance, which is a natural outcome of convergent type II migration (Snellgrove *et al.* 2001, Lee & Peale 2002, Kley *et al.* 2004, Kley *et al.* 2005), and secondly because under some circumstances (if the outer planet is sufficiently lightweight and barely opens a gap), the migration of the whole system may be reversed and be directed outwards (Masset & Snellgrove 2001, Morbidelli & Crida 2007, Zhang & Zhou 2008). Finally, as was first noted by Kley (2000) the distance between the giant planets brought to close

https://doi.org/10.1017/S1743921308016797 Published online by Cambridge University Press

orbits by convergent migration can be sufficiently short to render the system unstable after gas clearance, which may account for the eccentric orbits of some extrasolar planets.

4.3. *Type III migration*

Type III migration refers to a mode of migration for which the major driver is material flowing through the coorbital region. In the previous sections, the torque acting on a migrating planet was considered independent of its migration rate. However, the corotation torque implies material that crosses the planet orbit on the U-turn of the horseshoe streamlines. In a non-migrating case, only the material trapped in the horseshoe region participates in these U-turns, but in the case of an inward (or outward) migrating planet, material of the inner disk (outer disk) has to flow across the co-orbital region and executes one horseshoe U-turn to do so. By doing this, it exerts a corotation torque on the planet that scales with the drift rate. We call x_s the half radial width of the horseshoe region. The amount of specific angular momentum that a fluid element near the separatrix takes from the planet when it crosses the planet orbit and goes from the orbital radius $a - x_s$ to the orbital radius $a + x_s$ is $\Omega_p a x_s$. The corresponding torque exerted on the planet in steady migration is therefore, to lowest order in x_s/a:

$$\Gamma_2 = (2\pi a \Sigma_s \dot{a}) \cdot (\Omega_p a x_s), \tag{4.3}$$

where we keep the same notation as in Masset & Papaloizou (2003), hereafter MP03, and where Σ_s is the surface density at the upstream separatrix. As the system of interest, we take the system composed of the planet and all fluid elements trapped in libration in its co-orbital region, namely the whole horseshoe region (with mass M_{HS}) and the Roche lobe content (with mass M_R), because all of these parts perform a simultaneous migration. The drift rate of this system is then given by :

$$(M_p + M_{HS} + M_R) \cdot (a\dot{a}\Omega_p/2) = (4\pi a x_s \Sigma_s) \cdot (a\dot{a}\Omega_p/2) + \Gamma_{LR} \tag{4.4}$$

which can be rewritten as:

$$m_p \cdot (a\dot{a}\Omega_p/2) = (4\pi a \Sigma_s x_s - M_{HS}) \cdot (a\dot{a}\Omega_p/2) + \Gamma_{LR} \tag{4.5}$$

where $m_p = M_p + M_R$ is all the mass content within the Roche lobe, which for now on for convenience we refer to as the planet mass. The first term of the first bracket of the r.h.s. corresponds to the horseshoe region surface multiplied by the upstream separatrix surface density, hence it is the mass that the horseshoe region would have if it had a uniform surface density equal to the upstream surface density. The second term is the actual mass of the horseshoe region. The difference between these two terms is called in MP03 the coorbital mass deficit and denoted δm. Eq (4.5) yields a drift rate :

$$\dot{a} = \frac{\Gamma_{LR}}{2Ba(m_p - \delta m)} \tag{4.6}$$

This drift rate is faster than the standard estimate in which one neglects δm. This comes from the fact that the coorbital dynamics alleviates the task of the differential Lindblad torque by advecting fluid elements from the upstream to the downstream separatrix. The angular momentum they extract from the planet by doing so favors its migration. As δm tends to m_p, most of the angular momentum lost by the planet and its coorbital region is gained by the orbit crossing circulating material, making migration increasingly cost effective. When $\delta m \geqslant m_p$, the above analysis, assuming a steady migration ($\dot{a}$ constant), is no longer valid. Migration undergoes a runaway, and has a strongly time varying migration rate, that increases exponentially over the first libration

https://doi.org/10.1017/S1743921308016797 Published online by Cambridge University Press

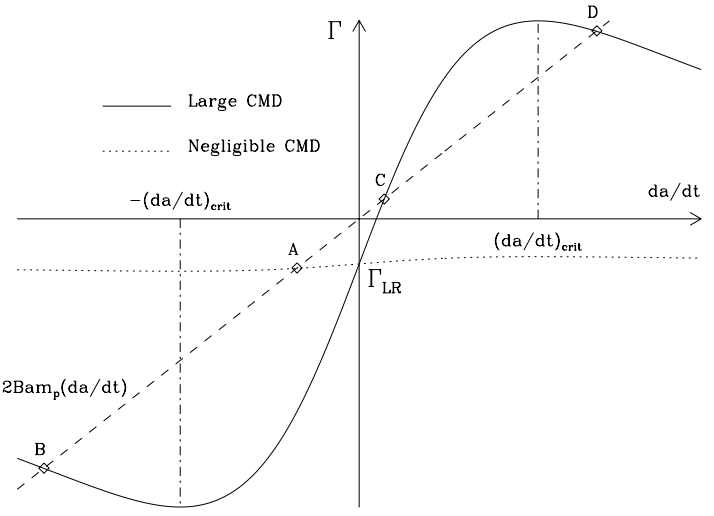

Figure 3. The solid curve shows the total torque on the planet in a massive disk (hence with a large coorbital mass deficit) as a function of the drift rate. For $|\dot{a}| \ll \dot{a}_{\rm crit}$ the torque exhibits a linear dependence in $\dot{a}$. The dotted line shows the torque in a low mass disk (i.e. with a negligible coorbital mass deficit), in which case the torque is almost independent of the migration rate and is always close to the differential Lindblad torque Γ_{LR}. The dashed line represents the planet angular momentum gain rate as a function of $\dot{a}$, assuming a circular orbit. For a given situation, the migration rate achieved by a steadily migrating planet is given by the intersection of the dashed line with the torque curve. In the low mass disk case, the intersection point, A, is unique, and stable. It yields a negative drift rate controlled by the differential Lindblad torque. In the high mass disk case (type III case), there are 3 points of intersection (B, C and D). The central point (C) is unstable, while the extreme ones (B and D) are stable and correspond to the maximum drift attained by the planet, either inwards (point B) or outwards (point D).

times. Runaway (also said type III) migration is therefore a mode of migration of planets that deplete their coorbital region and embedded in sufficiently massive disks, so that the above criterion be satisfied. An analysis similar to the above calculation may be performed, in which the corotation torque depends on the migration rate, except that one now has to introduce a delay τ between the mass inflow at the upstream separatrix and the corotation torque. Fluid elements passing through the upstream separatrix need indeed on average a fraction of a libration timescale to reach the planet and execute a horseshoe U-turn. This delay represents the latency of the feedback loop.

$$\Gamma_{CR}(t) = 2Ba\delta m\dot{a}(t-\tau) \tag{4.7}$$

A Taylor expansion in time of $\dot{a}(t-\tau)$ yields a first order differential equation for $\dot{a}$ (see MP03 for details). The linear dependence of the corotation on the drift rate remains valid as long as the semi-major axis variation over a horseshoe libration time is smaller than the horseshoe zone width, i.e.:

$$|\dot{a}| < \dot{a}_{\rm crit} = \frac{Ax_s^2}{2\pi a} \tag{4.8}$$

The corotation torque then reaches a maximum and slowly decays for larger values of $\dot{a}$ (see fig. 3).

https://doi.org/10.1017/S1743921308016797 Published online by Cambridge University Press

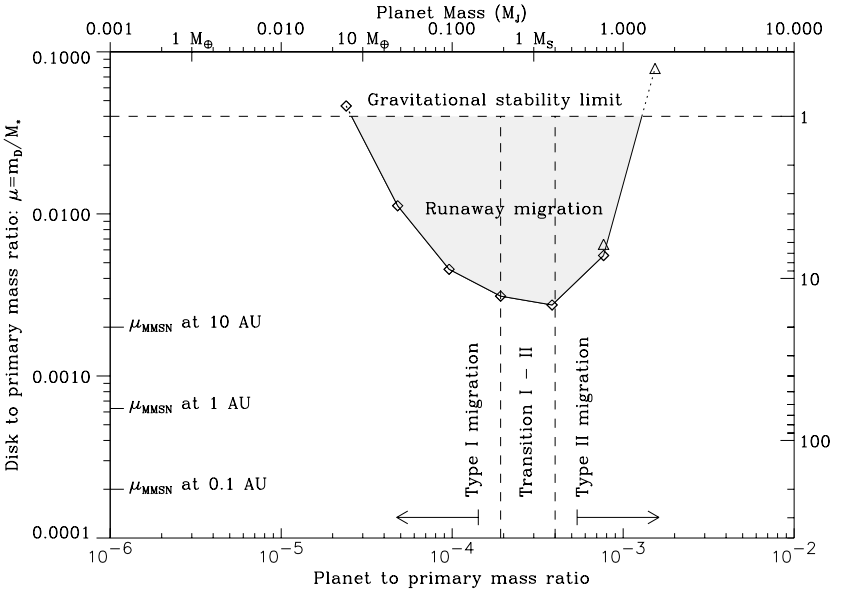

Figure 4. Runaway (or type III) limit domain for a $H/r = 0.04$ and $\nu = 10^{-5}$ disk, with a surface density profile $\Sigma \propto r^{-3/2}$. The variable $m_D = \pi\Sigma r^2$ features on the y axis. It is meant to represent the local disk mass, and it therefore depends on the radius. Type III is most likely for Saturn mass planets. These would undergo type III migration in disks no more massive than a few times the MMSN.

The terminal drift rate of a type III steadily migrating planet can be estimated by a standard bifurcation analysis as illustrated in fig. 3. The transition from one case to the other (one intersection point to three intersection points) occurs when the line showing the rate of change of the angular momentum (which has slope $am_p\Omega_p/2$) and the torque curve near the origin are parallel. Since this latter has a slope $a\delta m\Omega_p/2$ near the origin, the transition occurs near $m_p = \delta m$. The disk critical mass above which a planet of given mass undergoes a runaway depends on the disk parameters (aspect ratio and effective viscosity). The limit has been worked out by MP03 for different disk aspect ratios and a kinematic viscosity $\nu = 10^{-5}$. We reproduce in figure 4 the type III migration domain for a disk with $H/r = 0.04$.

A number of comments can be made from figure 4:

• The MMSN was barely massive enough to yield type III migration of Saturn. This suggests that in many protoplanetary disks, inferred to be several times more massive than the MMSN, type III migration is very likely for Saturn mass protoplanets.

• Type III is impossible for massive planets ($m_p > 1\ M_J$) as the horseshoe separatrices sample the gap edges in regions significantly depleted, yielding a small coorbital mass deficit.

• The sharp limit on the high mass side of the runaway domain might be related to the fact that most of the extrasolar planets known as "hot Jupiters", with a semi-major axis $a < 02.$ AU, happen to have sub-Jovian masses. A forming protoplanet, as it passes through the runaway domain, would migrate very fast towards the central object in a series of type III episodes, and at the same time it would accrete gas from the nebula. If the protoplanet happens to get out of the runaway domain before it reaches the central regions of the disk, it enters the slow, type II migration regime, having at least about a

https://doi.org/10.1017/S1743921308016797 Published online by Cambridge University Press

Jupiter mass. Otherwise, it may reach the central regions through type III migration (if the surface density profile is steep enough), still as a sub-Jovian object.

Type III migration, for the same disk profile and planet mass, can be directed either outwards or inwards, depending on the initial conditions. This is related to the fact that the differential equation obeyed by the semi-major axis, in the type III regime, is a second order differential equation in which one can specify independently a and $\dot{a}$. The type III migration of a planet therefore depends on its migration history, the "memory" of this history being stored in the way the horseshoe region is populated, i.e. in the repartition of the coorbital mass deficit. Note that owing to the strong variation of the drift rate in a type III episode, the horseshoe streamlines are not exactly closed, so that the coorbital mass deficit can be lost and type III migration can stall. This has been observed in numerical simulations, which show that the semi-major axis is varied by a factor of a few at most during a single type III episode.

4.4. *Stochastic migration*

Oftentimes, the protoplanetary disk is considered laminar while the accretion of material onto the central object is ensured by an *ad hoc* kinematic viscosity chosen to account for the mass accretion rate measured for T Tauri stars. The molecular viscosity of protoplanetary disks appears to be insufficient by many orders of magnitude, however, to reproduce the accretion rates typically measured. The source of the high effective viscosity in these disks is thought to be turbulence. The MRI (see section 4.2) has been identified as a powerful source of MHD turbulence in magnetized disks (Balbus & Hawley 1991, Hawley & Balbus 1991, Hawley & Balbus 1992), and this section will exclusively focus on the impact of this kind of turbulence on planetary migration.

MRI can develop only in regions of the disk where the matter and magnetic field are coupled, which requires a sufficiently high (albeit weak) ionization rate. In the planet-forming region ($1-10$ AU), it is thought that only the upper layers of the disk are ionized by X-rays from the central star or cosmic rays (Gammie 1996, Fromang *et al.* 2002). The bulk of the disk, however, should be ionized outside this region. This has led Gammie (1996) to the concept of layered accretion: the upper layers of the region between 1 and 10 AU participate in accretion onto the central star, whereas its magnetically inactive equatorial parts, usually called the *dead zone*, do not participate in the inwards flow of disk material.

There already exist a large number of works describing numerical simulations that self-consistently describe an MHD turbulent disk with embedded planets (Nelson & Papaloizou 2004, Papaloizou *et al.* 2004, Nelson & Papaloizou 2003, Nelson 2005, Winters *et al.* 2003). They exclusively consider a fully magnetized disk (hence with no dead zone), however, without any vertical stratification for reasons of computational cost.

Not surprisingly, the torque felt by a planet in a turbulent disk displays large temporal fluctuations. One can assign an order of magnitude to their amplitude by considering an overdense region of size H, located at a distance H from the planet such that the perturbed density in this region is of the same order as the unperturbed density. This yields an order of magnitude for the torque fluctuations of $G\Sigma a$ (Nelson & Papaloizou 2004, Nelson 2005).

Nelson and Papaloizou (2004) and Nelson (2005) have investigated the migration of low and intermediate mass planets embedded in turbulent disks. Laughlin *et al.* (2004) have also investigated this problem, but rather than tackling it through self-consistent numerical simulations they performed a two-dimensional calculation which mimicked the effects of turbulence using a time-varying, non-axisymmetric potential acting on the gas disk, rather than directly on the planet. The migration of low-mass planets embedded in

https://doi.org/10.1017/S1743921308016797 Published online by Cambridge University Press

turbulent disks is significantly different from the type I migration expected for laminar disks. The large torque variations due to turbulence induce the planet's semi-major axis to evolve on a random walk rather than systematically decay.

One question that is still open is whether the total torque felt by a planet in a turbulent disk can be decomposed into a laminar torque and the effect of fluctuations arising from the turbulence. We call the latter component the stochastic torque. One might expect that the time average of the stochastic torques is negligible compared to the total mean torque (which might be the same as the laminar torque, but this is still unknown), provided that this average is performed over a time interval that is much longer than the turbulence recurrence time. Under this assumption, the behavior of the planet should exhibit a systematic trend reminiscent of type I migration. Nelson (2005) has investigated the statistical properties of these torque fluctuations, finding significant power at low frequencies, corresponding to timescales comparable to the simulation time. As a consequence, in many of his calculations no systematic trend is observed; stochastic migration dominates type I migration over the entire run time of his calculations, or about 150 orbits. The reason for such significant power at very low frequencies is still unknown.

The amplitude of the specific stochastic torque is independent of the planet mass, whereas the specific wake torque scales with the planet mass. Nelson (2005) found that for planets up to $\sim 10\ M_\oplus$ the stochastic migration overcomes the systematic trend (over a simulation run time of 150 orbits), whereas systematic effects are dominant for larger masses. We mention however the recent work by Fromang & Nelson (2006), who argue that density fluctuations are smaller in a stratified, turbulent disk than in the unstratified models currently used to assess stochastic torques. This argument suggests that systematic effects could be dominant at masses even lower than $10\ M_\oplus$.

As pointed out by Johnson *et al.* (2006), if the turbulence has a finite correlation time then the stochastic (or diffusive) migration of low-mass planets can be reduced to an advection-diffusion equation. They show that diffusion always reduces the mean migration time of the planets, although a fraction of them still "survive" an extended period of migration.

5. Recent results on planetary migration

In the past few years, a number of new results have been obtained in the field of planetary migration either by the inclusion of new physical ingredients to the customary picture of planetary migration in a locally isothermal power law disk, or by intensive numerical modeling, or both. We draw hereafter a non comprehensive list of such results.

5.1. *Planetary migration and magnetic field*

Notwithstanding the issue of MRI and its non-linear outcome as MHD turbulence, the role of a toroidal or poloidal magnetic field on type I migration in a laminar disk as been contemplated by several authors. Terquem (2003) considers a disk threaded by a toroidal magnetic field, and shows that when the magnetic field as a function of radius decreases sufficiently fast, the total torque felt by the planet is positive, hence the planet migrates outwards. Fromang *et al.* (2005) have performed two-dimensional numerical simulations which essentially confirmed the analytic predictions of Terquem (2003). More recently, Muto *et al.* (2007, 2008) worked out the analytic torque expression both for a disk threaded by a poloidal magnetic field and a disk with a toroidal magnetic field, which enables them to make a variety of predictions about type I migration in magnetized disks.

5.2. *Inclusion of the disk's self gravity*

The protoplanetary disk's self-gravity, usually neglected on the grounds of its large Toomre parameter, has recently been contemplated by a number of authors, which were led to contradictory statements (Nelson & Benz 2003, Pierens & Huré 2005). Baruteau & Masset (2008a, 2008b) have revisited previous works on this subject and found that the inclusion of self-gravity slightly speeds up migration with respect to analytical drift rate estimates. They also exhibited a strong bias that systematically affects numerical calculations in which a planet is released and freely migrates in a non self-gravitating disk.

5.3. *Role of the corotation torque at a cavity edge*

Eq. (3.2) shows that the corotation torque can be a large, positive quantity at a surface density jump such that the surface density is larger on the outside, and that it may possibly overcome the differential Lindblad torque. This happens at a cavity edge, even if the cavity is shallow. This has led Masset *et al.* (2006) to the concept of planetary trap: type I migrating embryos are stopped whenever they reach a relatively abrupt drop of surface density, such as could be found at the inner edge of a dead zone, at the inner edge of a tidally truncated disk (Pierens & Nelson (2007)) or at the snow line (Zhang *et al.* 2008, Kretke *et al.* 2008).

5.4. *Planetary migration and radiative transfer*

Radiative transfer plays a very important role for planetary migration scenarios, for many different reasons. Menou and Goodman (2004) exploit the differential Lindblad torque's extreme sensitivity to the location of the Lindblad resonances. They consider realistic models of T Tauri α-disks instead of the customary power law models, and show that type I migration can be significantly slowed at opacity transitions. Jang-Condell and Sasselov (2005) argue that taking into account the temperature perturbations due to shadowing and irradiation of the disk photosphere could significantly reduce the type I migration rate. More recently, Paardekooper and Mellema (2006), hereafter PM06, consider a low-mass planet embedded in a disk with inefficient radiative cooling. A complex temperature structure develops in the vicinity of the planet which gives an underdense region behind the planet. As a consequence, the disk ultimately exerts a positive torque on the planet. This result clearly indicates that radiative transfer effects may prove crucial in resolving the problem of type I drift.

Baruteau and Masset (2008a, 2008b) have undertaken a follow up study of the results of PM06 in order to understand their physical origin. For this purpose, they considered the limiting case of a two dimensional, adiabatic flow. They firstly consider the linear case for an isolated resonance, for which they find an expression of the corotation torque which reduces to the usual dependence on the vortensity gradient in the limit of a cold disk. In the general case, they find an additional dependence on the entropy gradient at corotation. This dependence is associated to the advection of entropy perturbations. Secondly, they consider the case of a planet embedded in a Keplerian disk. They find, in the same manner, that the horseshoe drag contains a term that scales with the entropy gradient, and which may be strong enough to overcome the differential Lindblad torque, thus yielding a migration reversal. Although at the early stages of a calculation, the horseshoe drag's excess corresponds exactly to the series of torque excesses on individual corotation resonances, Paardekooper and Papaloizou (2007) argue that non-linear effects arise even at very low planetary mass and boost this excess with respect to its linear estimate. They further argue that the linearly estimated excess would be by itself not sufficient to halt migration. In any case, the self-consistent three dimensional calculation of PM06 shows that the migration of low-mass planets is reversed in the radiatively

https://doi.org/10.1017/S1743921308016797 Published online by Cambridge University Press

inefficient inner parts of protoplanetary disks. It will therefore be halted on the outer edge of this inner region. Paardekooper and Mellema (2007) estimate this location to be at $r \sim 10 - 15$ AU. Although the saturation properties of the corotation torque in a radiatively inefficient disk are still to be properly investigated, it is reasonable to expect that it remains unsaturated if the timescale for the relaxation of the temperature perturbations fulfills the following two requirements: (i) it is shorter than the horseshoe libration time (so that a nearly unperturbed entropy distribution reaches the horseshoe U-turns) (ii) it is longer than the horseshoe U-turn time, so that the flow can be considered as adiabatic over this timescale. Should these expectations be confirmed, this would provide a solution to the long-standing problem of type-I migration being too fast and flushing embryos onto the central object before they can accrete gas and become giant protoplanets.

6. Summary and discussion

Significant progress has been recently accomplished in the theories of planet-disk tidal interactions. Most of the new results have primarily been brought by large-scale calculations using modern supercomputer resources. In particular, the problem of type I migration is on the way of being solved, by relaxing the customary barotropic assumption, thereby enabling a new kind of perturbation (the so-called contact discontinuity familiar to the Riemann solvers community) to arise in the co-orbital region in the presence of an entropy gradient.

In the parts of a disk that are magnetically active, stochastic migration changes dramatically the migration properties of low- and intermediate-mass objects. Many questions remain open in this field which requires considerable computing resources.

The description of type II and type III migration also requires considerable computational resources. Primarily captured by simple two dimensional calculations in laminar disks, type II migration is now described by three dimensional hydrodynamics or magnetohydrodynamics calculations. An interesting problem, which has not yet been tackled, is the impact of gap edge irradiation on type II migration. In the same respect, while the physical picture of type III migration had been initially illustrated by two dimensional laminar calculations, an accurate description of its properties must be investigated by means of high resolution, three dimensional calculations. A first step forward has been made by Pepliński *et al.* (2007a, 2007b) who performed high resolution AMR two-dimensional calculations. A challenge for type III migration, whose onset depends on a subtle balance of gravitational and inertial effects, is to get rid of any possible artifact that may alter the effective inertial or gravitational mass of the migrating system (namely the planet and any fluid element trapped in libration with it, be it horseshoe or circumplanetary).

The actual trend among numericists performing calculations of planet-disk interactions is to include more and more physics relevant to planetary migration in their schemes. These efforts render scenarios of planetary migration progressively more quantitative and predictive, and they should in the future eventually bridge the gap between the properties of the protoplanetary disk, and the structure of the planetary systems that may emerge from it.

References

Artymowicz, P., 1993, *ApJ*, 419, 155
Balbus, S. A. & Hawley, J. F., 1991, *ApJ*, 376, 214

Baruteau, C. & Masset, F., 2008, *ApJ*, 672, 1054
Baruteau, C. & Masset, F., 2008, in: Y.-S. Sun, S. Ferraz-Mello & J.-L. Zhou, (eds.), *Exoplanets: Detection, Formation and Dynamics*, Proc. IAU Symposium No. 249 (Suzhou,China), p. 391
Bryden, G., Chen, X., Lin, D. N. C., Nelson, R. P., & Papaloizou, J. C. B., 1999, *ApJ*, 514, 344
Crida, A., Morbidelli, A., & Masset, F., 2006, *Icarus*, 181, 587
Fromang, S. & Nelson, R. P., 2006, *A&A*, 457, 343
Fromang, S., Terquem, C., & Balbus, S. A., 2002, *MNRAS*, 329, 18
Fromang, S., Terquem, C., & Nelson, R. P., 2005, *MNRAS*, 363, 943
Gammie, C. F., 1996, *ApJ*, 457, 355
Goldreich, P. & Tremaine, S., 1979, *ApJ*, 233, 857
Goldreich, P. & Tremaine, S., 1980, *ApJ*, 241, 425
Goodman, J. & Rafikov, R. R., 2001, *ApJ*, 552, 793
Hawley, J. F. & Balbus, S. A., 1991, *ApJ*, 376, 223
Hawley, J. F. & Balbus, S. A., 1992, *Bulletin of the American Astronomical Society* 24, 1234
Jang-Condell, H. & Sasselov, D. D., 2005, *ApJ*, 619, 1123
Johnson, E. T., Goodman, J., & Menou, K., 2006, *ApJ*, 647, 1413
Kley, W., 1999, *MNRAS*, 303, 696
Kley, W., 2000, *MNRAS*, 313, L47
Kley, W., Peitz, J., & Bryden, G., 2004, *A&A*, 414, 735
Kley, W., Lee, M. H., Murray, N., & Peale, S. J., 2005, *A&A*, 437, 727
Kretke, K. A. Lin, D. N. C., & Turner, N. J. 2008, in: Y.-S. Sun, S. Ferraz-Mello & J.-L. Zhou, (eds.), *Exoplanets: Detection, Formation and Dynamics*, Proc. IAU Symposium No. 249 (Suzhou,China), p. 293
Laughlin, G., Steinacker, A., & Adams, F. C., 2004, *ApJ*, 608, 489
Lee, M. H., & Peale, S. J., 2002, *ApJ*, 567, 596
Lin, D. N. C., Bodenheimer, P., & Richardson, D. C., 1996, *Nature* 380, 606
Lin, D. N. C. & Papaloizou, J., 1979, *MNRAS*, 186, 799
Lin, D. N. C. & Papaloizou, J., 1986, *ApJ*, 309, 846
Lin, D. N. C. & Papaloizou, J. C. B., 1993, in E. H. Levy & J. I. Lunine (eds.), *Protostars and Planets III*, pp 749–835
Lubow, S. H., Seibert, M., & Artymowicz, P., 1999, *ApJ*, 526, 1001
Masset, F., & Snellgrove, M., 2001, *MNRAS*, 320, L55
Masset, F. S. & Papaloizou, J. C. B., 2003, *ApJ*, 588, 494
Mayor, M., Queloz, D., Marcy, G., Butler, P., Noyes, R., Korzennik, S., Krockenberger, M., Nisenson, P., Brown, T., Kennelly, T., Rowland, C., Horner, S., Burki, G., Burnet, M., & Kunzli, M.: 1995, *IAU Circ.* 6251, 1
Menou, K. & Goodman, J., 2004, *ApJ*, 606, 520
Meyer-Vernet, N. & Sicardy, B., 1987, *Icarus*, 69, 157
Morbidelli, A., & Crida, A., 2007, *Icarus*, 191, 158
Muto T., Machida M., & Inutsuka, S., 2007, *ArXiv Astrophysics e-prints 0712.1060*
Muto, T., Machida, M. N., & Inutsuka, S.-I., 2008, in: Y.-S. Sun, S. Ferraz-Mello, & J.-L. Zhou, (eds.), *Exoplanets: Detection, Formation and Dynamics*, Proc. IAU Symposium No. 249 (Suzhou,China), p. 399
Nelson, A. F., & Benz, W., 2003, *ApJ*, 589, 556
Nelson, R. P., 2005, *A&A* 443, 1067
Nelson, R. P. & Papaloizou, J. C. B., 2003, *MNRAS*, 339, 993
Nelson, R. P. & Papaloizou, J. C. B., 2004, *MNRAS*, 350, 849
Nelson, R. P., Papaloizou, J. C. B., Masset, F. S., & Kley, W., 2000, *MNRAS*, 318, 18
Ogilvie, G. I. & Lubow, S. H., 2003, *ApJ*, 587, 398
Paardekooper, S. & Mellema, G., 2006, *A&A*, 459, 17
Paardekooper, S. & Mellema, G., 2007, *ArXiv Astrophysics e-prints 0711.3601, accepted by A&A*
Paardekooper, S. & Papaloizou, J., 2007, *submitted to A&A*
Papaloizou, J. C. B., Nelson, R. P., Kley, W., Masset, F. S., and Artymowicz, P., 2007, *Protostars and Planets V*, 655
Papaloizou, J. C. B., Nelson, R. P., & Snellgrove, M. D., 2004a, *MNRAS*, 350, 829

Papaloizou, J. C. B., Nelson, R. P., & Snellgrove, M. D., 2004b, *MNRAS*, 350, 829
Pepliński, A., Artymowicz, P., & Mellema, G., 2007a, *ArXiv Astrophysics e-prints 0709.3622, submitted to MNRAS*
Pepliński, A., Artymowicz, P., & Mellema, G., 2007b, *ArXiv Astrophysics e-prints 0709.3754, submitted to MNRAS*
Pierens, A., & Huré, J.-M., 2005, *A&A*, 433, L37
Pierens, A., & Nelson, R. P., 2007, *A&A*, 472, 993
Pollack, J. B., Hubickyj, O., Bodenheimer, P., Lissauer, J. J., Podolak, M., & Greenzweig, Y., 1996, *Icarus*, 124, 62
Snellgrove, M. D., Papaloizou, J. C. B., & Nelson, R. P., 2001, *A&A*, 374, 1092
Tanaka, H., Takeuchi, T., & Ward, W. R., 2002, *ApJ*, 565, 1257
Terquem, C. E. J. M. L. J., 2003, *MNRAS*, 341, 1157
Ward, W. R., 1986, *Icarus*, 67, 164
Ward, W. R., 1997, *Icarus*, 126, 261
Winters, W. F., Balbus, S. A., & Hawley, J. F., 2003, *ApJ*, 589, 543
Zhang, X. J., Kretke, K. A. Lin, & D. N. C. 2008, in: Y.-S. Sun, S. Ferraz-Mello & J.-L. Zhou, (eds.), *Exoplanets: Detection, Formation and Dynamics*, Proc. IAU Symposium No. 249 (Suzhou,China), p. 309
Zhang, H., & Zhou, J.-L. 2008, in: Y.-S. Sun, S. Ferraz-Mello & J.-L. Zhou (eds.), Exoplanets: Detection, Formation and Dynamics, Proc. IAU Symposium No. 249 (Suzhou, China), p. 413